

Simple and Accurate Analytical Model of Planar Grids and High-Impedance Surfaces Comprising Metal Strips or Patches

Olli Luukkonen, Constantin Simovski, *Member, IEEE*, Gérard Granet, George Goussetis, *Member, IEEE*, Dmitri Lioubtchenko, Antti V. Räisänen, *Fellow, IEEE*, and Sergei A. Tretyakov, *Fellow, IEEE*

Abstract

This paper introduces simple analytical formulas for the grid impedance of electrically dense arrays of square patches and for the surface impedance of high-impedance surfaces based on the dense arrays of metal strips or square patches over ground planes. Emphasis is on the oblique-incidence excitation. The approach is based on the known analytical models for strip grids combined with the approximate Babinet principle for planar grids located at a dielectric interface. Analytical expressions for the surface impedance and reflection coefficient resulting from our analysis are thoroughly verified by full-wave simulations and compared with available data in open literature for particular cases. The results can be used in the design of various antennas and microwave or millimeter wave devices which use artificial impedance surfaces and artificial magnetic conductors (reflect-array antennas, tunable phase shifters, etc.), as well as for the derivation of accurate higher-order impedance boundary conditions for artificial (high-) impedance surfaces. As an example, the propagation properties of surface waves along the high-impedance surfaces are studied.

I. INTRODUCTION

In this paper we consider planar periodic arrays of infinitely long metal strips and periodic arrays of square patches, as well as artificial high-impedance surfaces based on such grids. Possible applications for these arrays include artificial dielectrics [1], antenna radomes [2], other applications typical for frequency selective surfaces [3], and artificial high-impedance surfaces [4]–[8], where such arrays are located on a metal-backed dielectric layer (which may be perforated with metal vias). Furthermore, possible applications for artificial impedance surfaces expand the list to phase shifters [9], [10], TEM waveguides [11], planar reflect-arrays [12], absorbers [13]–[16], and artificial magnetic conductors (engineered antenna ground planes) [17]. Capacitive strips and square patches have been studied extensively in the literature (e.g., [18]–[20]). However, to the best of the authors' knowledge, there is no known easily applicable analytical model capable of predicting the plane-wave response of these artificial surfaces for large angles of incidence with good accuracy.

Models of planar arrays of metal elements excited by plane waves can be roughly split into two categories: computational and analytical methods. Computational methods as a rule are based on the Floquet expansion of the scattered field (see, e.g., [2], [3], [21], [22]). These methods are electromagnetically strict and general (i.e., not restricted to a particular design geometry). Periodicity of the total field in tangential directions allows one to consider the incidence of a plane wave on a planar grid or on a high-impedance surface as a single unit cell problem. The field in the unit cell of the structure can be solved using,

The work was supported in part by the Academy of Finland and Tekes through the Center-of-Excellence Programme.

O. Luukkonen, C. Simovski, D. Lioubtchenko, A. V. Räisänen and S. A. Tretyakov are with Department of Radio Science and Engineering/SMARAD CoE, TKK Helsinki University of Technology, P.O. 3000, FI-02015 TKK, Finland (email: olli.luukkonen@tkk.fi)

C. Simovski is also with Department of Physics, St. Petersburg Institute of Fine Mechanics and Optics, 197101, Sablinskaya 14, St. Petersburg, Russia.

G. Granet is with LASMEA, Université Blaise Pascal / CNRS, F-63177 Aubière Cedex, France

G. Goussetis is with the Institute of Integrated Systems, Edinburgh Research Partnership, Heriot-Watt University Edinburgh, EH14 AS, U.K.

for instance, the method of moments. However, in-house and commercial softwares using this technique consume considerable time and computational resources. This is restrictive in the design of complex structures where the array under study is only one of the building blocks. In these cases accurate and simple analytical models thrive, for they are easy to use and give good insight into physical phenomena.

For arrays of parallel capacitive strips located in a uniform host medium, one can find in [18] an equivalent circuit model valid for oblique incidence of TE- and TM-polarized waves. Patch arrays were not studied in [18]. In [21] it was shown that the accuracy of the model suggested in [18] is lost when the gap between the strips is not very small compared to the strip width. In [23] the authors derived averaged boundary conditions for planar arrays (in the first-order approximation, where the small parameter is the ratio period/wavelength). However, the oblique incidence case was not considered. In [24] a circuit model involving the so-called approximate Babinet principle (the conventional Babinet principle implies the location of two mutually complementing planar grids in a uniform background material) was developed for strips located at a dielectric interface. However, the analysis was restricted to the normal incidence as in [25] and [26]. In [25] and [26] periodical arrays of conducting wires on a dielectric interface were studied. In [27] the authors considered the reflection properties of arrays of separate scatterers (an array of square patches was studied as an example). The analysis was suitable for oblique incidence (see also in [28]); however, the model [27] is based on the assumption that the interaction of scatterers is the dipole interaction. Therefore, the accuracy of this model should be additionally studied for the case when the gaps separating the patches or strips are narrow, and the capacitive coupling between adjacent metal elements is strong. This situation holds for many frequency selective surfaces and for all high-impedance surfaces. When the effective capacitance of a planar array is high, the resonance frequency of a high-impedance surface comprising this array can be quite low. Structure miniaturization is practically equivalent to the decreasing of the resonance frequency of a structure with a given unit cell size. This target is always in mind of designers of microwave structures. In the present paper we will, in particular, consider the arrays with very small gaps between metal elements.

In [29] the expressions for the input impedances of high-impedance surfaces have been derived by treating the capacitive grid layer and the metal-backed dielectric slab with embedded vias as homogeneous materials with an anisotropic magneto-dielectric tensor. The resulting expressions for the input impedances are lengthy and complicated compared to the expressions of the present paper. While deriving semi-intuitively the expressions for the permittivities and permeabilities of the grid layer, the authors of [29] touch the topic of the grid impedance of arrays of patches without dealing with it in detail. In the present paper the grid impedance is derived strictly from the known expressions of the grid impedances for mesh of wires.

We start from the equivalent circuit model for arrays of parallel capacitive strips and square patches located on a dielectric interface. This model in the case of oblique incidence of plane waves is based on the so-called averaged boundary conditions (ABC). These conditions are derived below from the known averaged boundary conditions formulated earlier for parallel inductive strips and square strip meshes using the approximate Babinet principle (see e.g. [30]). The obtained results are compared to the ones found in the literature and to full-wave simulations. Then we will do the same for impenetrable impedance surfaces. This approach was already applied for the normal incidence in [5], and for the oblique incidence in [6], [7]. In [5] the authors studied the so-called mushroom structures [4]. In [6], [7] high-impedance surfaces were based on self-resonant grids (planar arrays of complex-shape elements). The accuracy for the oblique incidence offered by the analytical model for arrays of complex-shaped elements in [6], [7] was not high. Analytical calculations served in [6], [7] for heuristic purposes, and the Ansoft HFSS package was used for quantitative calculations. In the present paper we consider arrays of strips and patches and demonstrate the excellent accuracy of the simple approach based on the equivalent circuit, averaged boundary conditions, and the approximate Babinet principle. The reader should notice, that this approach was outlined in book [30] for arrays of metal patches. However, the results of [30] for grids of patches are not accurate for oblique incidence, because the periodicity in one of the tangential directions was not properly taken into account.

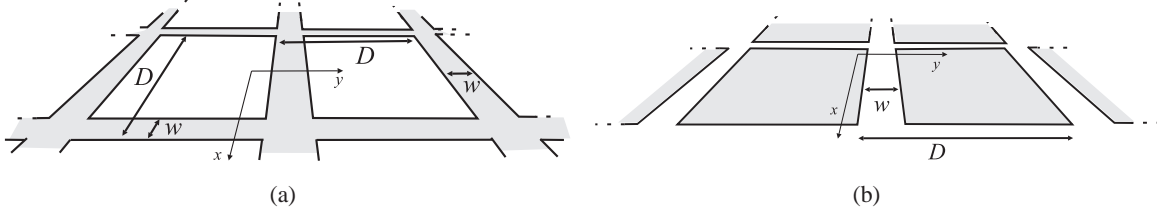


Fig. 1. (a) A mesh of ideally conducting strips in homogeneous host medium. (b) Array of patches in homogeneous host medium. Metal parts are colored grey.

II. GRID IMPEDANCE FOR CAPACITIVE STRIPS AND SQUARE PATCHES

A. Array of patches

First, we consider a mesh formed by laying parallel metallic strips along the x - and y -axes, as shown in Fig. 1(a). If the period D is electrically small, this structure is nearly isotropic and its electromagnetic response only weakly depends on the choice of the plane of incidence. As an example, assume incidence in the $(x - z)$ -plane. When $w \ll D$, where w is the width of the strips (see Fig. 1(a)), this grid can be considered as a mesh of strip wires with ideal contacts between crossing wires. When the electric field has a non-zero x - or y -component (parallel to the strips), the response of the grid is inductive at low frequencies. This response can be characterized by the so-called grid impedance, Z_g , which relates the averaged tangential component of the total electric field in the grid $(x - y)$ plane \hat{E}_x^{tot} or \hat{E}_y^{tot} to the averaged surface current density \hat{J} induced on it by the incident plane wave and flowing along the strips. For the TE-polarized case: $\hat{E}_y^{\text{tot}} = Z_g^{\text{TE}} \hat{J}_y$, where Z_g^{TE} is the grid impedance for the TE-polarized incidence wave and \hat{J}_y is the averaged surface current density along the y -axis. The averaging is made over the grid period D , and the current density \hat{J} is equal to the jump of the y - or x -component of the averaged magnetic field across the grid plane, respectively. The averaged boundary conditions for such meshes (derived by M.I. Kontorovich in the 1950s) can be found e.g. in [30]:

$$\hat{E}_x^{\text{tot}} = j \frac{\eta_{\text{eff}}}{2} \alpha \left[\hat{J}_x + \frac{1}{k_{\text{eff}}^2 (1 + \frac{b}{D})} \frac{b}{D} \frac{\partial^2}{\partial x^2} \hat{J}_x \right], \quad (1)$$

$$\hat{E}_y^{\text{tot}} = j \frac{\eta_{\text{eff}}}{2} \alpha \hat{J}_y, \quad (2)$$

for TM- and TE-polarized incident fields, respectively. In the above formulae b and D are the periods of the structure along the x - and y -axes, respectively, $\eta_{\text{eff}} = \sqrt{\mu_0 / \varepsilon_0 \varepsilon_{\text{eff}}}$ is the wave impedance of the uniform host medium with relative effective permittivity ε_{eff} in which the grid is located, and α is called the *grid parameter* [30]. In our isotropic case $D = b$. Furthermore, $k_{\text{eff}} = k_0 \sqrt{\varepsilon_{\text{eff}}}$ is the wave number of the incident wave vector in the effective host medium. μ_0 , ε_0 , and k_0 are the permeability, permittivity, and the wave number in free space, respectively.

Though relations (1) and (2) were obtained for the case when the host medium is uniform, we heuristically extend it to the case when the grid is located on a surface of a dielectric substrate with the relative permittivity ε_r . The effective permittivity of an equivalent uniform medium in (1) and (2) in this case can be approximated as [24]:

$$\varepsilon_{\text{eff}} = \frac{\varepsilon_r + 1}{2}. \quad (3)$$

The grid parameter for an electrically dense ($k_{\text{eff}} D \ll 2\pi$) array of ideally conducting strips reads [30]:

$$\alpha = \frac{k_{\text{eff}} D}{\pi} \ln \left(\frac{1}{\sin \frac{\pi w}{2D}} \right), \quad (4)$$

where w is the strip width. For cases when $w \ll D$, the natural logarithm in relation (4) can be approximated as $\ln\left(\frac{2D}{\pi w}\right)$. A more accurate approximation for the grid parameter taking into account terms of the order $\left(\frac{k_0 D}{\pi}\right)^5$ and oblique incidences can be found in [31]. It has been shown in that paper that for sparse wire grids the accuracy of the higher order approximation is very good up to the frequencies when $D = \lambda$. Over this limit the phase variations on the surface are too rapid and averaging fails. At higher frequencies grating lobes emerge (i.e. higher Floquet space harmonics become propagating) and anyway a single impedance would not suffice for the description of the properties of the surface.

Replacing $\frac{\partial}{\partial x}$ by $-jk_x$, where $k_x = k_0 \sin \theta$ (θ is the angle of incidence and $k_y = 0$) is the x -component of the incident wave vector in the free space, we obtain from (1) and (2) the grid impedances in the form:

$$Z_g^{\text{TM}} = j \frac{\eta_{\text{eff}}}{2} \alpha \left(1 - \frac{k_0^2 \sin^2 \theta}{k_{\text{eff}}^2} \right), \quad (5)$$

$$Z_g^{\text{TE}} = j \frac{\eta_{\text{eff}}}{2} \alpha. \quad (6)$$

Here, TM and TE refer to the TM- and TE-polarized incident fields, respectively. Now we can derive the grid impedance for the complementary structure, that is, for an array of patches (see Fig. 1(b)). To find its grid impedance we use the approximate Babinet principle (e.g. [25], [30]) which reads in terms of grid impedances as:

$$Z_g^{\text{TE}} Z_{g'}^{\text{TM}} = \frac{\eta_{\text{eff}}^2}{4}, \quad (7)$$

where $Z_{g'}^{\text{TM}}$ is the grid impedance of the complementary structure for TM-polarized incidence fields. Similarly, the grid impedance of the complementary structure for TE-polarized incident fields is obtained through the Babinet principle and Z_g^{TM} . Applying the approximate Babinet principle we have from (5) and (6):

$$Z_{g'}^{\text{TM}} = -j \frac{\eta_{\text{eff}}}{2\alpha}, \quad (8)$$

$$Z_{g'}^{\text{TE}} = -j \frac{\eta_{\text{eff}}}{2\alpha \left(1 - \frac{k_0^2 \sin^2 \theta}{k_{\text{eff}}^2} \right)}. \quad (9)$$

If the plane of incidence for the mesh of strips in Fig. 1(a) for the TE-polarized incident wave is the $(x - z)$ plane, then (following from the Babinet principle) for the array of patches in Fig. 1(b) for the TE-polarized incident field the plane of incidence is the $(y - z)$ plane.

B. Arrays of strips

Periodical grid of perfectly conducting strips whose width w is much smaller than the distance $D - w$ between the adjacent strips (we again restrict the study by this case) is shown in Fig. 2(a) (current flows along the strips). The expression for the grid impedance for both TE- and TM-polarizations for this case can be found in [30]. The complementary structure of Fig. 2(a) is shown in Fig. 2(b) (current flows across the strips). Let the electric field of the incident wave be x -polarized in Fig. 2(a). Then for the TM-polarized wave the incidence plane is the $(x - z)$ plane ($k_y = 0$) and for the TE-polarized wave the incidence plane is the $(y - z)$ plane ($k_x = 0$). For the grid depicted in Fig. 2(b) the electric field is parallel to the y axis. The TE polarization corresponds to the incidence plane $(x - z)$ and the TM polarization corresponds to the incidence plane $(y - z)$.

From (7) and from the expressions for the grid impedances for the structure depicted in Fig. 2(a) (e.g. from [30]) we get the grid impedance of the capacitive grid of strips for both polarizations:

$$Z_{g'}^{\text{TM}} = -j \frac{\eta_{\text{eff}}}{2\alpha}, \quad (10)$$

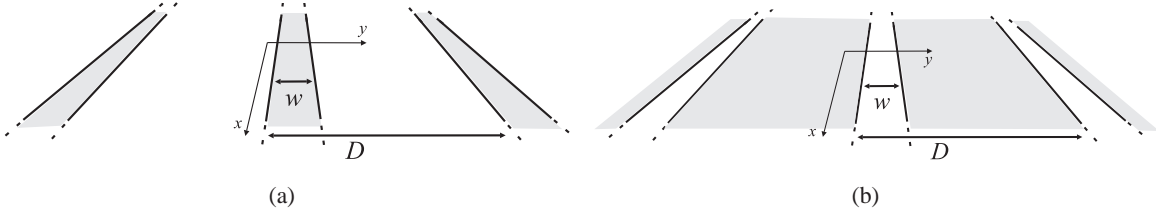


Fig. 2. (a) An inductive grid of metal strips in homogeneous host medium. (b) A capacitive grid of metal strips in homogeneous host medium. Metal parts are colored grey.

$$Z_{g'}^{\text{TE}} = -j \frac{\eta_{\text{eff}}}{2\alpha} \frac{1}{\left(1 - \frac{k_0^2}{k_{\text{eff}}^2} \sin^2 \theta\right)}. \quad (11)$$

These results correspond to those available in [18]. The structures presented in Figs. 1(b) and 2(b) have equivalent grid impedance for the TM-polarized incident wave. For the TE polarization the grid impedances of the capacitive grid of parallel strips differs from that of the patch array due to the factor $\frac{1}{2} \sin^2(\theta)$ in (9) instead of $\sin^2(\theta)$ in (11) in the denominator.

C. The reflection and transmission coefficients of patch arrays

The equivalent circuit that can be used to calculate the reflection and transmission coefficient from an array of patches with a certain corresponding grid impedance $Z_{g'}$ is shown in Fig. 3(a) (see also e.g. in [18]). The transmission-line model for a high-impedance surface in Fig. 3(b) will be discussed in the following section. The free space impedances, Z_0 , for the TE and TM modes are given for different angles of incidence as:

$$Z_0^{\text{TE}} = \frac{\eta_0}{\cos \theta}, \quad (12)$$

$$Z_0^{\text{TM}} = \eta_0 \cos \theta, \quad (13)$$

where η_0 is the plane wave impedance in free space. The input (surface) impedance referring to the illuminated surface of the grid $Z_{\text{inp}}^{\text{TE, TM}}$ is a parallel connection of the grid impedance $Z_{g'}$ and Z_0 :

$$Z_{\text{inp}}^{-1} = Z_{g'}^{-1} + Z_0^{-1}. \quad (14)$$

From (8) and (9) we have for the case of an array of patches in free space:

$$Z_{g'}^{\text{TM}} = -j \frac{\eta_0}{2\alpha}, \quad Z_{g'}^{\text{TE}} = -j \frac{\eta_0}{2\alpha \left(1 - \frac{\sin^2 \theta}{2}\right)}. \quad (15)$$

The angular dependency of the grid impedance in the TE-polarized case for an array of patches located

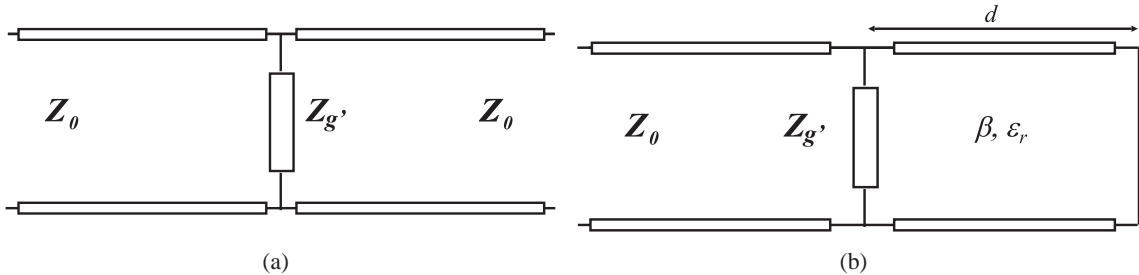


Fig. 3. (a) The transmission-line model for a capacitive grid of strips or an array of patches in free space. (b) The transmission-line model for a high-impedance surface comprising a grid of capacitive strips or an array of patches on top of a metal-backed dielectric slab. The expressions for Z_0 and $Z_{g'}$ are given in (12), (13), and (15).

in free space in (15) is different from the predictions of the known analytical model developed in [27]. In [27] the reflection coefficients for the TE- and TM-polarized cases are presented. The grid impedances corresponding to the reflection coefficient in [27] would read:

$$Z_H^{\text{TE, TM}} = -j \frac{\eta}{2a}, \quad (16)$$

where

$$a = kD \frac{0.51 \left(\frac{D-w}{D}\right)^3}{1 - 0.367 \left(\frac{D-w}{D}\right)^3}. \quad (17)$$

The suffix H refers here to Holloway et al. [27]. Apart from different approximations for the grid parameter, the analytical results presented by Eqs. (15) and (16) have clearly different angular dependencies. In order to compare the accuracy of the two models, in the following subsection we evaluate the predictions of our analytical models and those in [27] against full-wave simulation results.

D. Numerical validation

Here we compare the analytical results obtained using the present model and the model in [27] with simulations. The numerical simulations are based on the Floquet expansion (the Fourier modal method developed in [32] and used in [33] for analysis of strip gratings). In Fig. 4 the results obtained using the Fourier modal method are denoted as Fourier results. In all of the numerical simulations the periodical structures were considered to be infinite.

The reflectance of the patch array for the TE- and TM-polarized incident fields is shown in Fig. 4. The reflection coefficients have been calculated using the transmission-line model in Fig. 3(a) and (15). In Fig. 4 the results correspond to the dimensions $D = \lambda/10$ and $w = D/10$. The analytical results are compared with the results according to (16). These results are denoted by R_H in Fig. 4. The present analytical model shows very good agreement with the numerical results, whereas the alternative analytical model [27] appears to be significantly less accurate.

III. HIGH-IMPEDANCE STRUCTURES

A. Input impedance of high-impedance surfaces

The high-impedance surfaces (HIS) studied here consist of the above considered capacitive grids or arrays on a metal-backed dielectric slab with thickness d and relative permittivity ϵ_r . In Fig. 5 a HIS with a patch array is shown. Similarly, one can realize a HIS with parallel capacitive strips. The input (surface)

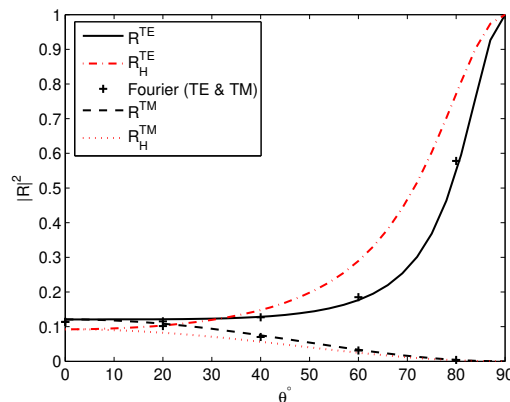


Fig. 4. Color online. The TE- and TM-reflection coefficient versus the incident angle for an array of square patches. The dimensions of the array are the following: $D = \lambda/10$ and $w = D/10$. R_H corresponds to the results according to the model by C. L. Holloway et al. [27].

impedance of the HIS can be understood if we look at Fig. 3(b). In Fig. 3(b) β is the propagation constant component orthogonal to the surface. The input (surface) impedance is a parallel connection of the grid impedance $Z_{g'}$ and the surface impedance of the grounded dielectric layer Z_s :

$$Z_{\text{inp}}^{-1} = Z_{g'}^{-1} + Z_s^{-1}. \quad (18)$$

The surface impedance for the oblique incidence can be written in the dyadic form (see e.g. in [30]) which splits into two scalars Z_s^{TE} and Z_s^{TM} in the TE- and TM-cases, respectively:

$$\overline{\overline{Z}}_s = j\omega\mu \frac{\tan(\beta d)}{\beta} \left(\overline{\overline{I}}_t - \frac{\mathbf{k}_t \mathbf{k}_t}{k^2} \right), \quad (19)$$

where μ is the absolute permeability of the substrate (in our case $\mu = \mu_0$), $\beta = \sqrt{k^2 - k_t^2}$, $k = k_0 \sqrt{\epsilon_r}$ is the wave number in the substrate material, and \mathbf{k}_t is the tangential wave number component, as imposed by the incident wave.

For a HIS comprising capacitive strips the TM- and TE-input impedances follow from Eqs. (10), (11) and (19), and read, respectively:

$$Z_{\text{c,inp}}^{\text{TM}} = \frac{j\omega\mu \frac{\tan(\beta d)}{\beta} \cos^2(\theta_2)}{1 - 2k_{\text{eff}}\alpha \frac{\tan(\beta d)}{\beta} \cos^2(\theta_2)}, \quad (20)$$

$$Z_{\text{c,inp}}^{\text{TE}} = \frac{j\omega\mu \frac{\tan(\beta d)}{\beta}}{1 - 2k_{\text{eff}}\alpha \frac{\tan(\beta d)}{\beta} \left(1 - \frac{2}{\epsilon_r + 1} \sin^2 \theta \right)}, \quad (21)$$

where θ is the angle of incidence and θ_2 is calculated from the law of refraction as:

$$\theta_2 = \arcsin \left(\frac{\sin(\theta)}{\sqrt{\epsilon_r}} \right). \quad (22)$$

In the case of patch arrays, the input impedances follow from Eqs. (8), (9) and (19). For the TM-polarization the input impedance equals to that of (20). For the TE-polarization the input impedance reads:

$$Z_{\text{p,inp}}^{\text{TE}} = \frac{j\omega\mu \frac{\tan(\beta h)}{\beta}}{1 - 2k_{\text{eff}}\alpha \frac{\tan(\beta h)}{\beta} \left(1 - \frac{1}{\epsilon_r + 1} \sin^2 \theta \right)}. \quad (23)$$

In the case of electrically thin substrates the expressions for the input impedances can be further simplified by replacing the $\tan(\beta h)$ by its argument βh . In addition, the substrate losses can be taken into account in the analytical model simply by replacing the relative permittivity with an appropriate complex number. However, the effect of losses have been considered to be out of the scope of this paper. Therefore in the following part the validation of the model for HIS is conducted for lossless structures.

B. Numerical validation

Since the HIS is impenetrable, in the absence of losses its reflectance is equal to unity for the frequency range considered here. Therefore the analytical model is verified from the reflection phase diagrams for

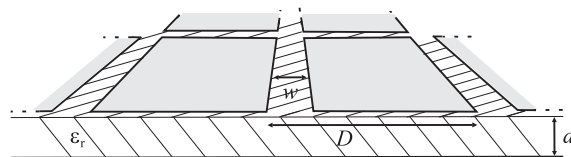


Fig. 5. A high-impedance structure consisting of an array of patches on top of a metal-backed dielectric slab.

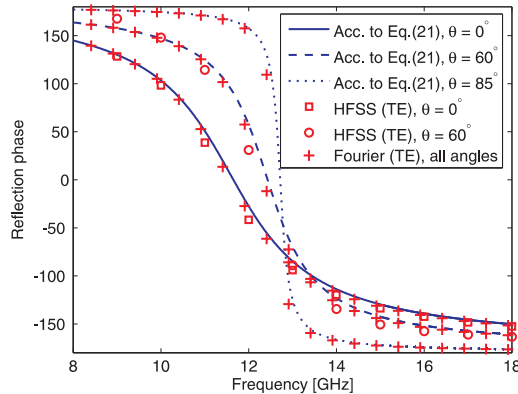


Fig. 6. Color online. The reflection phase diagram for TE-polarized incident fields for a high-impedance surface consisting of capacitive strips for different angles of incidence. The parameters of the high-impedance surface are the following: $D = 2$ mm, $w = 0.2$ mm, $d = 1$ mm, and $\varepsilon_r = 10.2$. HFSS simulations were not done for $\theta = 85^\circ$.

different angles of incidence. Our analytical expressions are compared to the results of two accurate full-wave simulations: Ansoft's High Frequency Structure Simulator 10.1.1. (HFSS) and the Fourier modal method. In addition we have compared our analytical expressions and the results of MoM simulations in the case of square patches.

In Figs. 6 and 7 the reflection phase diagram is presented for the TE- and TM-polarized incident fields, respectively. It corresponds to a HIS comprising capacitive strips on top of a dielectric slab grounded by a perfectly conducting plane. The parameters of the HIS are the following: $D = 2$ mm, $w = 0.2$ mm, $d = 1$ mm, and $\varepsilon_r = 10.2$.

For the HIS comprising an array of square patches analogous results are shown in Figs. 8 and 9. The numerical parameters of this HIS are the same as those in the previous example. The agreement between the analytical and numerical results is very good for all angles of incidence. The HIS comprising an array of patches was simulated also with HFSS for the incidence angles of 0° and 60° . The results of the HFSS simulations showed excellent agreement with the analytical and Fourier results. Figures 6–9 show that the present analytical model is perfectly adequate for lossless HIS comprising capacitive patch and strip arrays.

Let us define the resonant bandwidth of the HIS in the reflection phase diagrams as the frequency band in which the reflection phase is from -90° to 90° . It is clear that in Figs. 6–9 the resonant bandwidth of the TM (TE) polarized wave is increased (decreased) as the angle of incidence increases. Although the surface impedance of the HIS changes with respect to the incident angle, it does not explain this behavior. This is rather due to the fact that the free space surface impedances in (12) and (13) and their proportion to the surface impedance of the HIS increase or decrease as the incident angle is increased, respectively, when calculating the reflection coefficient.

For frequencies higher than 20 GHz the HIS with the chosen parameters cannot be homogenized and we cannot expect our model to be adequate in this range. Using a more accurate approximation for the grid parameter [31] the validity range of our model could be extended. However, we cannot predict higher-order surface impedance resonances with our model and the limits of the model have not been studied here. Nevertheless, within the frequency band of the main (lowest) resonance the present model has been shown to be very accurate for all angles of incidence up to nearly grazing incidence.

IV. SURFACE WAVES

Knowledge about surface waves along the impedance surfaces is needed when using the impedance surfaces as leaky wave antennas [34], artificial magnetic conductors for antenna applications [20], or to suppress back radiation of the antennas [22]. In this section the propagation properties of surface waves

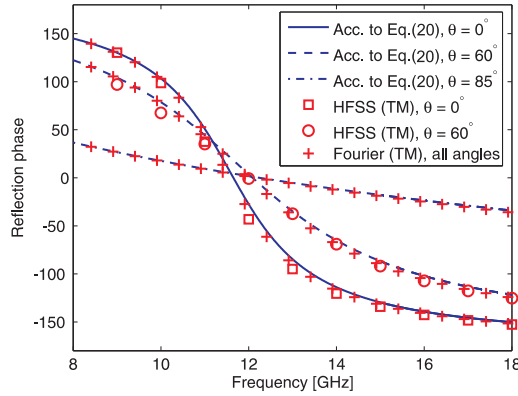


Fig. 7. Color online. The reflection phase diagram for TM-polarized incident field for a high-impedance surface consisting of capacitive strips for different angles of incidence. The parameters of the high-impedance surface are the following: $D = 2$ mm, $w = 0.2$ mm, $d = 1$ mm, and $\varepsilon_r = 10.2$. HFSS simulations were not done for $\theta = 85^\circ$.

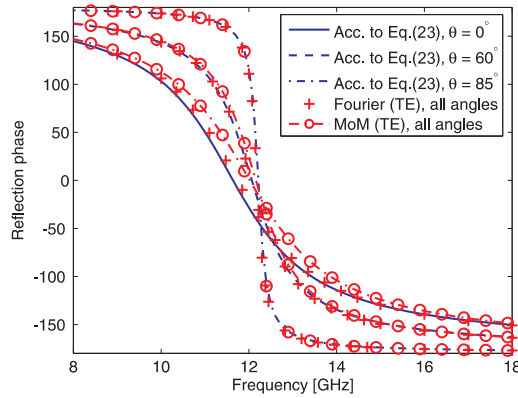


Fig. 8. Color online. The reflection phase diagram for TE-polarized incident field for a high-impedance surface consisting of square patches for different angles of incidence. The dimensions of the high-impedance surface are the following: $D = 2$ mm, $w = 0.2$ mm, $d = 1$ mm, and $\varepsilon_r = 10.2$.

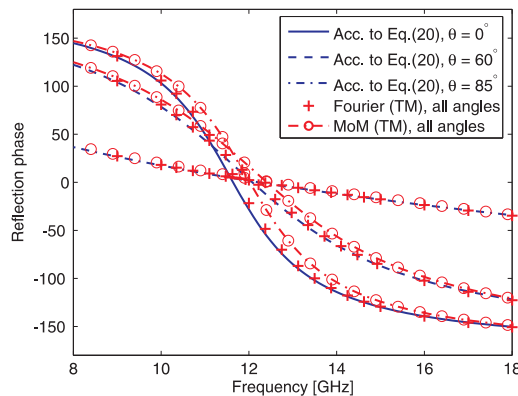


Fig. 9. Color online. The reflection phase for TM-polarized incident field for a high-impedance surface consisting of square patches for different angles of incidence. The dimensions of the high-impedance surface are the following: $D = 2$ mm, $w = 0.2$ mm, $d = 1$ mm, and $\varepsilon_r = 10.2$.

along a HIS are studied.

The derived expressions for the input impedance of the HIS can be used for analysis of the surface

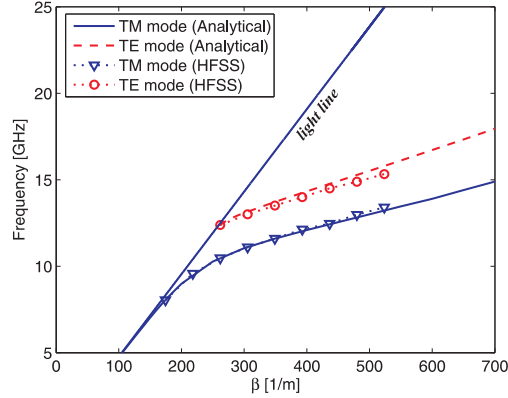


Fig. 10. Color online. The propagation properties of the surface waves along the example HIS. The dimensions of the high-impedance surface are the following: $D = 2$ mm, $w = 0.2$ mm, $d = 1$ mm, and $\epsilon_r = 10.2$.

wave propagation. Here we only study the propagation of surface waves along the HIS surface comprising an array of patches. The propagation properties of the surface waves can be calculated from the transverse resonance condition (e.g. [35]):

$$Z_0^{-1} + Z_{p,\text{inp}}^{-1} = 0, \quad (24)$$

where Z_0 is the free-space impedance given in (12) and (13) for TE- and TM-polarized incident fields, respectively, and the input impedance of the surface $Z_{p,\text{inp}}$ is given in (20) and (23) for TM- and TE-polarized incident fields, respectively. In the absence of losses $Z_{p,\text{inp}}$ is purely imaginary. In this case Z_0 needs to be purely imaginary in order for (24) to be true. This means that the angle of incidence in (12) and (13) needs to be imaginary, that is, $\cos(\theta) = \frac{\sqrt{k_0^2 - k_t^2}}{k_0}$ and $k_t > k_0$ (waves along the z -axis in free space need to attenuate).

As an example, the dispersion of surface waves propagating along the HIS studied in the previous section are shown in Fig. 10. The dimensions of the HIS are the following: $D = 2$ mm, $w = 0.2$ mm, $d = 1$ mm, and $\epsilon_r = 10.2$. The simulations have been done with HFSS 10.1.1 for an infinite structure. The analytical results agree very well with the simulated results.

V. CONCLUSIONS

In this paper we have considered two types of planar capacitive grids of metal elements separated by thin slits from one another, namely grids of strips and arrays of square patches. The equivalent grid impedance for the arrays of square patches has been derived. We have shown that the grid impedance for strips and patches have different angular dependencies. The obtained expressions based on the transmission-line approach and the Babinet principle have been thoroughly checked using both commercial simulation software and in-house numerical codes based on the full-wave equations. Careful comparison have demonstrated that the present model agrees with results of [29] and is more accurate compared to the other previously reported analytical models. We must emphasize here that the Fourier Modal Method allows the increase of the spatial resolution around the edges of the strips or patches, where a singularity of the field occurs. As a consequence, the algorithm does not suffer from instability. It follows from this that, while checking the convergence of the results carefully, 21 Floquet harmonics in one direction are enough to obtain good accuracy with this method.

Furthermore, we have applied these analytical results for high-impedance surfaces, where a planar grid is located over a grounded dielectric layer. Here the comparison with the exact solutions allowed us to check the assumption that the same grid impedance as derived for the uniform host medium can be applied when the grid is located at a dielectric interface (using the concept of the effective permittivity). For two types of HIS under study the verification against numerical results has demonstrated very good agreement

in the frequency range of the main surface resonance, where the HIS operates as an artificial magnetic conductor. This conclusion is true for both polarizations and all angles of incidence up to nearly grazing incidence. It has also been shown in this paper that the proposed model for high-impedance surfaces allows very accurate prediction of the surface wave propagation for both polarizations. The present study allows us to conclude that the simple transmission-line model combined with the approximate Babinet principle and the assumption of effective uniform permittivity (when calculating the grid impedance of the capacitive array) is, in fact, a very accurate model for these high-impedance surfaces.

ACKNOWLEDGEMENTS

The work was supported in part by the Academy of Finland and Tekes through the Center-of-Excellence Programme. Olli Luukkonen wishes to thank the Nokia Foundation for financial support and acknowledge Dr. Sergey Dudorov for useful discussions.

REFERENCES

- [1] S. B. Cohn, "Dielectric properties of a lattice of anisotropic particles," *J. Appl. Phys.*, Vol. 27, pp. 1106–1107, 1956.
- [2] C. C. Chen, "Transmission through a conducting screen perforated periodically with apertures," *IEEE Trans. Microwave Theory Tech.*, Vol. MTT-18, pp. 627–632, 1970.
- [3] B. A. Munk, *Frequency Selective Surfaces: Theory and Design*. Wiley: New York, 2000.
- [4] D. Sievenpiper, L. Zhang, R. F. J. Broas, N. G. Alexopoulos, and E. Yablonovich, "High-impedance electromagnetic surfaces with a forbidden frequency band," *IEEE Trans. Microwave Theory Tech.*, Vol. 47, pp. 2059–2074, 1999.
- [5] S. A. Tretyakov and C. R. Simovski, "Dynamic model of artificial reactive impedance surfaces," *J. of Electromagn. Waves and Appl.*, Vol. 17, No. 1, pp. 131–145, 2003.
- [6] C. R. Simovski and A. A. Sochava, "High-impedance surfaces based on self-resonant grids. Analytical modelling and numerical simulations," *Progress in Electromagnetics Research*, PIER 43, pp. 239–256, 2003.
- [7] C. R. Simovski, P. de Maagt, and I. V. Melchakova, "High-impedance surface having stable resonance with respect to polarization and incidence angle," *IEEE Trans. Antennas Propag.*, Vol. 53, No. 3, pp. 454–460, 2005.
- [8] S. Maci and P.-S. Kildal, "Hard and soft surfaces realized by FSS printed on a grounded dielectric slab," *IEEE Antennas and Propagation Society International Symposium, 2004*, Vol. 1, pp. 285–288, 2004.
- [9] J. A. Higgins, H. Xin, A. Sailer, and M. Rosker, "Ka-band waveguide phase shifter using tunable electromagnetic crystal sidewalls," *IEEE Trans. Microwave Theory Tech.*, Vol. 51, No. 4, pp. 1281–1287, April 2003.
- [10] D. Chicherin, S. Dudorov, D. Lioubtchenko, V. Ovchinnikov, S. Tretyakov, and A. Räisänen, "MEMS-based high-impedance surfaces for millimeter and submillimeter wave applications," *Microw. Opt. Tech. Lett.*, Vol. 48, No. 12, pp. 2570–2573, Dec. 2006.
- [11] F.-R. Yang, K.-P. Ma, Y. Qian, and T. Itoh, "A novel TEM waveguide using uniplanar compact photonic-bandgap (UC-PBG) structure," *IEEE Trans. Microwave Theory Tech.*, Vol. 47, No. 11, pp. 2092–2098, Nov. 1999.
- [12] D. F. Sievenpiper, J. H. Schaffner, H. Jae Song, R. Y. Loo, and G. Tangonan, "Two-dimensional beam steering using an electrically tunable impedance surface," *IEEE Trans. Antennas Propag.*, Vol. 51, No. 10, pp. 2713–2722, Oct. 2003.
- [13] N. Engheta, "Thin absorbing screens using metamaterial surfaces," in *Dig. 2002 IEEE AP-S Int. Symp.*, San Antonio, TX, vol. 2, pp. 392–395, 2002.
- [14] S. A. Tretyakov and S. I. Maslovski, "Thin absorbing structure for all incident angles based on the use of a high-impedance surface," *Microw. Opt. Tech. Lett.*, Vol. 38, No. 3, pp. 175–178, 2003.
- [15] Q. Gao, Y. Yin, D.-B. Yan, and N.-C. Yuan, "A novel radar-absorbing-material based on EBG structure," *Microw. Opt. Tech. Lett.*, Vol. 47, No. 3, pp. 228–230, 2005.
- [16] S. Simms and V. Fusco, "Thin absorber using artificial magnetic ground plane," *Elect. Lett.*, Vol. 41, No. 24, pp. 1311–1313, 2005.
- [17] D. Sievenpiper, "High-impedance electromagnetic surfaces," Ph.D. Dissertation, Univ. California, Dept. Elect. Eng., Los Angeles, CA, 1999.
- [18] N. Marcuvitz (ed.), *Waveguide Handbook*, IEE Electromagnetic Waves Series 21, (McGraw-Hill, New York, 1951), p. 218, 280.
- [19] S.-W. Lee, G. Zarrillo, and C.-L. Law, "Simple formulas for transmission through periodic metal grids or plates," *IEEE Trans. Antennas Propag.*, Vol. AP-30, No. 5, pp. 904–909, Sep. 1982.
- [20] G. Goussettis, A. P. Feresidis, and J. C. Vardaxoglou, "Tailoring the AMC and EBG characteristics of periodic metallic arrays printed on grounded dielectric substrate," *IEEE Trans. Antennas Propag.*, Vol. 54, No. 1, pp. 82–89, 2006.
- [21] K. W. Whites and R. Mittra, "An equivalent boundary-condition for lossy periodic structures at low frequencies," *IEEE Trans. Antennas Propag.*, Vol. 44, No. 12, pp. 1617–1629, Dec. 1996.
- [22] S. Maci, M. Caiazzo, A. Cucini, and M. Casaletti, "A pole-zero matching method for EBG surfaces composed of a dipole FSS printed on a grounded dielectric slab," *IEEE Trans. Antennas Propag.*, Vol. 53, No. 1, pp. 70–81, Jan. 2005.
- [23] R. R. DeLyser and E. F. Kuester, "Homogenization analysis of electromagnetic strip gratings," *J. of Electromagn. Waves and Appl.*, Vol. 5, No. 11, pp. 1217–1236, 1991.
- [24] R. C. Compton, L. B. Whitbourn, and R. C. McPherdan, "Strip gratings at a dielectric interface and application of Babinet's principle," *Appl. Opt.*, Vol. 23, No. 18, pp. 3236–3242, Sep. 1984.
- [25] L. B. Whitbourn and R. C. Compton, "Equivalent-circuit formulas for metal grid reflectors at a dielectric boundary," *Appl. Opt.*, Vol. 24, No. 2, pp. 217–220, 1985.

- [26] R. Ulrich, "Far-infrared properties of metallic mesh and its complementary structure," *Infrared Phys.*, Vol. 7, pp. 37–55, 1967.
- [27] C. L. Holloway, M. A. Mohammed, and E. F. Kuester, "Reflection and transmission properties of a metafilm: With an application to a controllable surface composed of resonant particles," *IEEE Trans. Electromagn. Compat.*, Vol. 47, No. 4, pp. 853–865, 2005.
- [28] E. F. Kuester, M. A. Mohammed, M. Piket-May, and C. L. Holloway, "Averaged transition conditions for electromagnetic fields at a metafilm," *IEEE Trans. Antennas Propag.*, Vol. 51, No. 10, pp. 2641–2651, 2003.
- [29] S. Clavijo, R. E. Díaz, and W. E. McKinzie, III, "High-impedance surfaces: An artificial magnetic conductor for a positive gain electrically small antennas," *IEEE Trans. Antennas Propag.*, Vol. 51, No. 10, pp. 2678–2690, 2003.
- [30] S. A. Tretyakov, *Analytical Modeling in Applied Electromagnetics*, Artech House: Norwood, MA, 2003.
- [31] V. V. Yatsenko, S. A. Tretyakov, S. I. Maslovski, and A. A. Sochava, "Higher order impedance boundary conditions for sparse wire grids," *IEEE Trans. Antennas Propag.*, Vol. 48, No. 5, pp. 720–727, 2000.
- [32] G. Granet and J.-P. Plumey, "Parametric formulation of the Fourier modal method for crossed surface-relief gratings," *J. Opt. A*, Vol. 4, No. 5, pp. S145–S149, 2002.
- [33] G. Granet and B. Guizal, "Analysis of strip gratings using a parametric modal method by Fourier expansions," *Opt. Commun.*, Vol. 255, No. 1–3, pp. 1–11, 2005.
- [34] D. F. Sievenpiper, "Forward and backward leaky wave radiation with large effective aperture from an electronically tunable textured surface," *IEEE Trans. Antennas Propag.*, Vol. 53, No. 1, pp. 236–247, 2005.
- [35] T. Rozzi and M. Mongiardo, *Open Electromagnetic Waveguides*, IEE Electromagnetic Waves Series 43, (IEE, London, 1997).